

This is an electronic reprint of the original article. This reprint may differ from the original in pagination and typographic detail.

---

## Coculture of *P. aeruginosa* and *S. aureus* on cell derived matrix - An in vitro model of biofilms in infected wounds

Gounani, Zahra; Şen Karaman, Didem; Venu, Arun P.; Cheng, Fang; Rosenholm, Jessica M.

*Published in:*  
Journal of Microbiological Methods

*DOI:*  
[10.1016/j.mimet.2020.105994](https://doi.org/10.1016/j.mimet.2020.105994)

Published: 01/08/2020

*Document Version*  
Accepted author manuscript

*Document License*  
CC BY-NC-ND

[Link to publication](#)

*Please cite the original version:*  
Gounani, Z., Şen Karaman, D., Venu, A. P., Cheng, F., & Rosenholm, J. M. (2020). Coculture of *P. aeruginosa* and *S. aureus* on cell derived matrix - An in vitro model of biofilms in infected wounds. *Journal of Microbiological Methods*, 175, Article 105994. <https://doi.org/10.1016/j.mimet.2020.105994>

### General rights

Copyright and moral rights for the publications made accessible in the public portal are retained by the authors and/or other copyright owners and it is a condition of accessing publications that users recognise and abide by the legal requirements associated with these rights.

### Take down policy

If you believe that this document breaches copyright please contact us providing details, and we will remove access to the work immediately and investigate your claim.

1 **Coculture of *P. aeruginosa* and *S. aureus* on cell derived matrix -**  
2 **an *in vitro* model of biofilms in infected wounds**

3 **Zahra Gounani\*<sup>1,2</sup>, Didem Şen Karaman<sup>3</sup>, Arun P. Venu<sup>4</sup>, Fang Cheng<sup>4,5</sup>, Jessica. M.**  
4 **Rosenholm\*<sup>1</sup>**

5 1. Pharmaceutical Sciences Laboratory, Faculty of Science and Engineering, Åbo Akademi  
6 University, Turku 20520, Finland

7 2. Physics, Faculty of Science and Engineering, Åbo Akademi University, Turku 20500,  
8 Finland

9 3. Biomedical Engineering Department, Faculty of Engineering and Architecture, İzmir  
10 Katip Çelebi University, İzmir, Turkey

11 4. Cell Biology, Biosciences, Faculty of Science and Engineering, Åbo Akademi University,  
12 Turku 20520,

13 5. School of Pharmaceutical Sciences (Shenzhen), Sun Yat-sen University, Guangzhou,  
14 510006, China

15 **Corresponding authors:**

16 **Zahra Gounani**

17 *Current address:*

18 Physics/Åbo Akademi University

19 Gadolinia (2nd floor)

20 Porthaninkatu 3, FI - 20500 Turku, Finland

21 E-mail: [zahra.gounani@abo.fi](mailto:zahra.gounani@abo.fi)

22 **Jessica M. Rosenholm**

23 Pharmacy/Åbo Akademi University

24 BioCity (3rd floor)

25 Tykistökatu 6A, FI - 20520 Turku, Finland

26 E-mail: [jessica.rosenholm@abo.fi](mailto:jessica.rosenholm@abo.fi)

27

## 28 **Abstract**

29 Polymicrobial biofilms are major complications of various chronic infections. Therefore, *in*  
30 *vitro* biorelevant polymicrobial biofilm models are essential tools for medical studies. This  
31 study presents a dual species biofilm of *Pseudomonas aeruginosa* and *Staphylococcus aureus*  
32 developed on cell-derived matrices (CDMs), in order to simulate the microenvironment of *in*  
33 *vivo* biofilms. *P. aeruginosa* and *S. aureus* are two of the most frequent pathogens in  
34 polymicrobial biofilms of wound infections. Although they are commonly isolated from  
35 polymicrobial biofilms, their interaction is antagonistic; and there is severe battle between them  
36 for nutrients and space. We introduced a nutritious formulation supporting co-cultures of *P.*  
37 *aeruginosa* and *S. aureus* in order to study the interaction of these gram-positive and gram-  
38 negative bacterial species. Quantitative analyses demonstrated that the enrichment of tryptic  
39 soy broth (TSB) with NaCl and glucose facilitate dual-species biofilm formation of *P.*  
40 *aeruginosa* and *S. aureus* when it is mixed with fetal bovine serum (FBS). Furthermore, the  
41 dual species biofilm was incubated on CDMs. Characterization of the model by fluorescent  
42 and electron microscopies revealed realistic features of chronic multi-species biofilms,  
43 including competitive distribution pattern of two bacterial species and small-colony variants  
44 (SCVs) morphology of *S. aureus*.

45

46 **Keywords;** Dual-species biofilm, Cell derived matrix, Biofilm model, *Pseudomonas*  
47 *aeruginosa*, *Staphylococcus aureus*.

## 48 **1. Introduction**

49 Wound management is a well-established clinical practice; however, chronic wounds remain  
50 one of the major health issues and count for significant morbidity and mortality all over the  
51 world. Chronic wounds include diabetic ulcers, pressure ulcers, venous leg ulcers and burn  
52 wounds, and these affect 6.5 million people only in the U.S annually (Han and Ceilley, 2017).  
53 It is estimated that chronic wound care cost 2-3% of the healthcare budget in developed  
54 countries, and wound healing accounts for a market exceeding US\$27 billion (Frykberg and  
55 Banks, 2015; Han and Ceilley, 2017). Chronic wounds are formed when the wound healing  
56 process fails to progress orderly and stall in one phase, usually the inflammatory phase  
57 (Frykberg and Banks, 2015). It occurs as a result of molecular events such as excessive ROS  
58 production, increased stimulation of proteases, and secretion of inflammatory cytokines; all of  
59 which cause an extended inflammatory stage (McCarty and Percival, 2013). Microbial biofilms  
60 are also considered as one of the main causes of wound chronicity, although it is yet to be  
61 proved by the medical community (Sun et al., 2008). Biofilms are often polymicrobial, i.e.  
62 consisting of different species, such as *Staphylococcus*, *Pseudomonas*, *Enterococcus*, *Proteus*  
63 and several others (Lipsky and Hoey, 2009).

64 *In vitro* and *in vivo* models are essential elements of medical studies and drug development  
65 research (Sahlgren et al., 2017). *In vivo* models provide more realistic data, but has the  
66 disadvantages of being expensive and are subject to ethical dilemmas associated with animal  
67 research (Mathes et al., 2014). *Ex vivo* models provide close *in vivo* resemblance, but the  
68 variability of the tissues between different donors, availability limits, and complexity of the  
69 tissue restricts their applications (Mathes et al., 2014). Therefore, *in vitro* models are one of  
70 the key requirements to obtain predictive data before *in vivo* and clinical evaluation (Mathes et  
71 al., 2014). An appropriate *in vitro* biofilm model should offer *in vivo* relevant characteristics  
72 while being rapid, non-expensive and easy to set up (Kucera et al., 2014) There are previous

73 studies reporting on multispecies biofilm models, for example, Sun *et al.* developed an  
74 outstanding multispecies model from three different bacterial species of *Pseudomonas*  
75 *aeruginosa*, *Enterococcus faecalis*, and *Staphylococcus aureus* (Sun et al., 2008). In another  
76 study, the authors used a similar model to study the dynamics of population of each species  
77 during biofilm formation by selective culture and qPCR (Kucera et al., 2014). However, these  
78 studies developed multi-species biofilms on solid surfaces which are lack of *in vivo* features  
79 and microenvironment. Werthen *et al.* developed mono-species biofilm model on a matrix of  
80 collagen (Werthe et al., 2010). Although they avoided using solid surface to grow biofilms,  
81 their model did not include the complex features of polymicrobial biofilms.

82 In this study, a dual species biofilm of *Staphylococcus aureus* and *Pseudomonas aeruginosa*  
83 was generated on cell-derived matrices (CDMs) as a major component of wound bed, to  
84 provide a more biorelevant biofilm model. CDMs are decellularized extracellular matrices  
85 (ECM) which are comprised of highly organized assemblies of macromolecules including  
86 collagen, fibronectin, laminin, glycosaminoglycans, proteoglycans and matricellular proteins  
87 (Fitzpatrick and McDevitt, 2015). ECM is the largest constituent of the skin layers and play a  
88 major role in the wound healing process (Magana et al., 2018). ECM create structural and  
89 functional integrity for the wound bed, and influence all physiological and structural  
90 interactions of wound components and biofilm residents (Zeng et al., 2015). CDMs have been  
91 recently developed and used successfully in designing cell cultural substrates and tissue  
92 engineered products (Fitzpatrick and McDevitt, 2015). Using CDMs as substrate for growing  
93 biofilms, we expected to recreate a more relevant microenvironment of *in vivo* biofilms.

94 *P. aeruginosa* and *S. aureus* both are opportunistic species and the most common residents of  
95 polymicrobial biofilms in chronic wounds (DeLeon et al., 2014). The co-presence of *P.*  
96 *aeruginosa* and *S. aureus* cause delayed and improper wound healing and trigger worse  
97 outcomes for patients (Hotterbeekx et al., 2017). *P. aeruginosa* and *S. aureus* are also the most

98 isolated bacterial species in cystic fibrosis (CF) patients (Laura M. Filkins et al., 2015). Despite  
99 the fact that they are common co-colonizing pathogens in most infections, *in vitro* cocultures  
100 of *P. aeruginosa* and *S. aureus* is problematic, as *P. aeruginosa* eradicate *S. aureus* already in  
101 the first hours of incubation (DeLeon et al., 2014). The killing effect of *P. aeruginosa* on *S.*  
102 *aureus* has been attributed to different extracellular factors secreted by *P. aeruginosa*,  
103 including anti-Staphylococcal 4-Hydroxy-2-Heptylquinoline N-Oxide (HQNO), Pyocyanin  
104 and LasA protease (Hotterbeekx et al., 2017). To develop a cost-effective and appropriate  
105 growth media in which co-cultured biofilm formation of *P. aeruginosa* and *S. aureus* is  
106 supported, we modified tryptic soy broth (TSB) with FBS, NaCl and glucose. The existence of  
107 dual species in the biomimetic biofilm model was characterized by different imaging methods.  
108 The presented method to provide dual species biofilm growth on CDMs can be ascribed as a  
109 pioneering effort to create phenotype of complex *in vivo* biofilms with the observable traits,  
110 including the biochemical and physiological properties.

## 111 **2. Material and Methods**

### 112 **2.1. Growth kinetic of bacterial species in different broths**

113 *Pseudomonas aeruginosa* (PAO1 DSM 19880) and *Staphylococcus aureus* (ATCC 25923)  
114 were stored at -70°C and restored on tryptic soy agar plates (TSA, Sigma Aldrich Co., St.  
115 Louis, MO). Single colonies of each bacterial species from agar plates were grown in tryptic  
116 soy broth (TSB), Mueller Hinton broth (MHB) and Luria-Bertani (LB) for 20 h at 37 °C (in 50  
117 ml falcon tubes containing 10 ml media, the caps of which were loosed for aeration). The day  
118 after, overnight culture was diluted (10: 10000) and allowed to grow for another 24 hours.  
119 Growth kinetic of both bacterial species were determined in different media, taking 100 µl of  
120 culture at 0, 2, 4, 8, and 24 h for colony forming units (CFU) numeration on the agar plates by  
121 dilution plating method. All experiments were carried out with two replicates. For each

122 replication 5-6 dilutions were cultured on corresponding agar plates. The total number of  
123 colonies ( $\log_{10}$  CFU ml<sup>-1</sup>) was counted after 20 h of incubation at 37 °C.

## 124 **2.2. Dual species biofilm formation**

125 Dual species biofilm was grown in a medium made by mixing TSB and fatal bovine serum  
126 (FBS) (1: 1). TSB was used as it is or TSB supplemented with 1% glucose (TSBG), 2.5% NaCl  
127 (TSBN), 1% NaCl (TSBn), 1% glucose + 1% NaCl (TSBGn), 1% glucose + 2.5% NaCl  
128 (TSBGN). To prepare overnight culture, single colony of each bacteria was grown in TSB (10  
129 ml) overnight (20 h) at 37 °C and 180 rpm. Then overnight culture was diluted (1000-fold) in  
130 TSB and incubated at 37°C and 180 rpm for 4 hours. Microtiter polystyrene 96-well assay  
131 plates (Thermo Scientific, Nunclon) and matching peg-lids (Thermo Scientific, Nunclon) were  
132 used to grow biofilm. Each well was filled up with 149  $\mu$ l of TSB or enriched TSBs with NaCl  
133 and glucose as described earlier. Aliquots from 4 hours culture of *S. aureus* (10  $\mu$ l) and *P.*  
134 *aeruginosa* (1  $\mu$ l) was added to each well to a final volume of 160  $\mu$ l/well. Final concentration  
135 of both *S. aureus* and *P. aeruginosa* in each well was  $\sim 10^7$  CFU/ml. Non-inoculated media was  
136 used as negative control. All experiments were carried out in four replicates. Plate was then  
137 incubated at 37°C for 20 h. The day after, peg-lid was removed. Liquid culture containing  
138 planktonic bacteria was transferred to another plate for CFU counting. Both biofilms formed  
139 on pegs and plate wells were washed with PBS 3 times, to remove loosely attached bacteria.  
140 The biofilm in plate wells were dispersed in 160  $\mu$ l/well fresh media before CFU counting.  
141 Peg-lid was transferred to new plate containing 160  $\mu$ l/well fresh media (recovery plate). To  
142 retrieve bacterial cell of biofilm to liquid media, first grown biofilm around pegs was gently  
143 scrapped using sterile pipette tip and then peg-lid with recovery plate was sonicated for 3  
144 minutes. To enumerate CFU, 100  $\mu$ l aliquots of each well was taken to a 10 fold serial dilution  
145 and 3 $\times$ 10  $\mu$ l of five last dilution was plated on MacConkey agar (MCK) plates, as selective  
146 media for *P. aeruginosa* and mannitol salt agar (MSA) plates, as selective media for *S. aureus*.

147 MCK and MSA plates were incubated at 37°C for 24 h and 48 h, respectively. After completion  
148 of incubation time, colonies were counted and log<sub>10</sub> CFU/ml values were plotted versus time.

### 149 **2.3. Developing cell derived matrices (CDMs):**

150 CDMs was prepared based on a method reported before with minor modification(Kaukonen et  
151 al., 2017). Glass cover slips (diameter, 11 mm) were placed in 24 well plates after sterilization  
152 with 70% ethanol. Sterile solution of gelatin (0.2% w/v in sterile PBS) was pre-warmed at 37  
153 °C and added to each well (800 µl) and incubated for 1 h at 37 °C or 24 h at 4 °C. Then gelatin  
154 solution was aspirated, and cover slips were washed with PBS gently. Gelatin coating of cover  
155 slip then was crosslinked using aqueous solution of glutaraldehyde (1% v/v, 500 µl) for 30 min  
156 at room temperature (RT). The crosslinking solution was then removed, and cover slips were  
157 washed with PBS two times. Remaining glutaraldehyde were quenched by 500 µl glycine  
158 solution (in PBS, 1 M) for 20 min at RT. After removing glycine solution, coverslips were  
159 washed with PBS and incubated in pre-warmed Dulbecco's modified eagle's medium (DMEM)  
160 media (800 µl) at 37 °C for 1 hour. Then fibroblast cells were cultured on cover slips ( $5 \times 10^4$   
161 per well) at 37 °C. The cells were allowed to grow until they formed a confluent monolayer.  
162 Then, growth media was removed and replaced with supplemented DMEM media with 50 µg  
163 ml<sup>-1</sup> ascorbic acid. Ascorbic acid stock was prepared freshly (by dissolving ascorbic acid  
164 powder in growth media) and was filtered using a 0.45-µm filter. The ascorbic acid treatment  
165 was done every other day and continued for 14 to 21 days. After completion of ascorbic acid  
166 treatment, the media was removed, and cells were washed by PBS. Fibroblast cells were then  
167 denuded by an extraction solution (500 µl per well), made by mixing 1 ml of NH<sub>4</sub>OH, 250 µl  
168 of Triton X-100 and 48.75 ml of PBS. The extraction solution was pre-warmed before using  
169 and incubated with cells about 2 minutes, until cells were all detached. Then the extraction  
170 solution was removed gently from the wells and cell were washed with PBS twice. The final  
171 step of CDMs preparation, is removing cellular DNA by DNase I. A solution of DNase I was

172 prepared in deionized water ( $10 \mu\text{g ml}^{-1}$ ) and was added to each well (500  $\mu\text{l}$ ). The plate was  
173 incubated at 37 °C for 30 min. Finally, DNase solution was removed and CDMs were washed  
174 with PBS twice. CDMs were stored in PBS buffer containing 1% (vol/vol) penicillin–  
175 streptomycin at 4 °C until further use (up to 4 weeks).

#### 176 **2.4. Dual species biofilm formation on CDMs**

177 To develop dual species biofilm on CDMs, enriched TSB with 1% glucose + 2.5% NaCl  
178 (TSBGN) mixed with FBS (50: 50) was used. CDMs were placed in 24-well plates and were  
179 washed with PBS two times. 800  $\mu\text{l}$  of mixed media inoculated with  $10^7$  and  $10^6$  CFU/ml of *S.*  
180 *aureus* and *P. aeruginosa* was added to each well. Wells without CDMs filled with inoculated  
181 media and non-inoculated were used as positive and negative control. The plates were then  
182 incubated at 37 °C for 20 h before CFU enumeration. The experiments were performed in four  
183 replicates. After 20 h, planktonic growth removed from the wells and biofilm was washed by  
184 PBS three times to remove loose bacteria. Then Biofilm was dispersed in media. The CFU  
185 number of biofilms on CDMs were determined by culturing serially diluted of bacterial biofilm  
186 on selective media of MCK and MSA for *P. aeruginosa* and *S. aureus*, respectively.

#### 187 **2.5. Fluorescent staining of dual-species biofilm on CDMs:**

188 Live/dead viability staining assay was employed to visualize live and dead cells in dual-species  
189 biofilm on surface of CDMs. Grown biofilm on surface of CDMs was washed with PBS three  
190 times. A mixture of syto 9 ( $2 \mu\text{gml}^{-1}$ ) and propidium iodide ( $10 \mu\text{gml}^{-1}$ ) in PBS (500  $\mu\text{l}$ ) was  
191 added to each sample and incubated for 30 minutes in RT before imaging. Images were  
192 obtained using Zeiss LSM780 confocal laser microscopy (Jena, Germany), by Plan-  
193 Apochromat 63x/1.40 Oil immersion objective, and excitation with 488 nm and 543 nm lasers.

## 194 **2.6. Immunofluorescence staining of CDMs:**

195 Extracellular matrix are usually visualized by immunofluorescence staining of their fibrillary  
196 proteins(Kaukonen et al., 2017). Here, collagen and fibronectin organizations were  
197 immunostained to visualize CDMs. CDMs were fixed in formalin 10% (500  $\mu$ l) for 15 min at  
198 room temperature. Then fixative was removed and CDMs were washed with PBS twice. Horse  
199 serum 30% (v/v in PBS) was added to CDMs as blocking solution and left for 15 min at room  
200 temperature. Horse serum was replaced with primary antibody solution (10  $\mu$ g ml<sup>-1</sup> in horse  
201 serum 30%) and incubated for 1 h at room temperature. We used collagen (rabbit anti-collagen  
202 I, Novus NB600-408) and fibronectin (rabbit anti-fibronectin, Sigma Aldrich F3648)  
203 antibodies. Then primary antibodies were replaced with secondary antibody, Alexa Fluor 488  
204 (green, donkey anti-rabbit), and incubated for another 1 hour at room temperature. Then,  
205 secondary antibody solution was removed and CDMs were washed with PBS three times and  
206 with deionized water once. For CDM covered by biofilm, after removing secondary antibody  
207 a solution of propidium iodide (PI) 10  $\mu$ l/ml was added to each well and plate was incubated  
208 for 30 minutes at room temperature before washing with PBS and deionized water. The excess  
209 water was drained by touching a piece of filter paper. Finally, CDMs were mounted on glass  
210 slide by Mowiol (7  $\mu$ l) and were let dry for 24 hours before imaging. Slides were imaged by a  
211 Zeiss LSM780 (Jena, Germany) using a Plan-Apochromat 63x/1.40 Oil immersion objective,  
212 and excitation with 488 nm and 543 nm lasers.

## 213 **2.7. Scanning electron microscopy (SEM)**

214 SEM analysis was performed to study the surface morphology of CDMs and dual-species  
215 biofilm on the surface of CDMs. CDMs with or without biofilm were washed 5 times with PBS  
216 very gently. Then all samples were fixed with formalin 10% for 15 min at room temperature.  
217 After removing formalin, CDMs were washed with PBS three times and with deionized water

218 once and left to dry overnight. Dried samples were mounted on sample holders, and sputter  
219 coated with carbon. Scanning electron microscopy (SEM) was performed with a LEO Gemini  
220 1530® (Zeiss, Oberkochen, Germany) with a Thermo Scientific UltraDry Silicon Drift  
221 Detector (SDD).

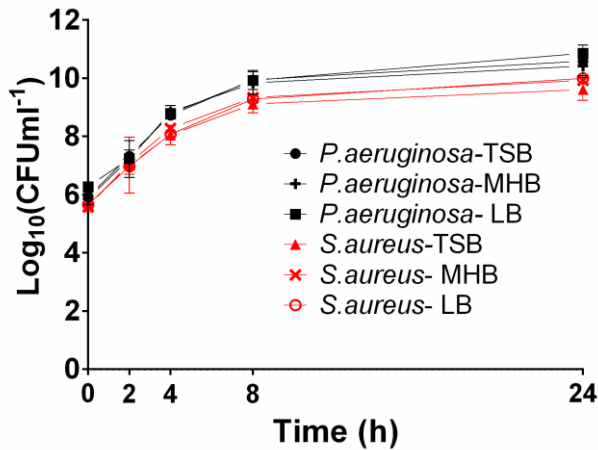
### 222 **3. Results and Discussion**

223 Our goal with this study was to develop an *in vivo* relevant model of wound biofilms by  
224 growing dual-species biofilm on cell derived matrixes (CDMs). Our criteria for the model were  
225 as follows: 1) developing a dual-species biofilm model involving both gram-negative and  
226 gram-positive bacteria; 2) growing the biofilm in a growth media made of inexpensive and  
227 readily available materials in bacterial cell labs; 3) using CDMs as substrate for growing  
228 biofilms to provide an *in vivo* like microenvironment for biofilms.

#### 229 **3.1. Growth kinetics of bacterial species in different broths**

230 We first followed the growth profile of each bacteria in different common bacterial growth  
231 media (Fig 1). Growth curve of bacteria was obtained by CFU counting at different time points  
232 as shown in Fig. 1. In all three media, *P. aeruginosa* showed higher growth rate. Then, a wide  
233 range of media mixtures were screened to grow dual species biofilms; however, they all failed  
234 in growing *S. aureus* in the presence of *P. aeruginosa* (data not shown). *P. aeruginosa* tend to  
235 outcompete or kill *S.aureus* in *in vitro* cocultures (Filkins *et al*, 2015; Hotterbeekx *et al*, 2017).

236



237

238 Figure 1: Growth kinetic of *P. aeruginosa* and *S. aureus* in three different media. Results  
 239 revealed that growth rate of *P. aeruginosa* was slightly higher than *S. aureus* at the 24 h time  
 240 point, while their growth rates were almost the same in other time points. Error bars indicate  
 241 standard deviation (SD) from the mean of the 2 biological replicates.

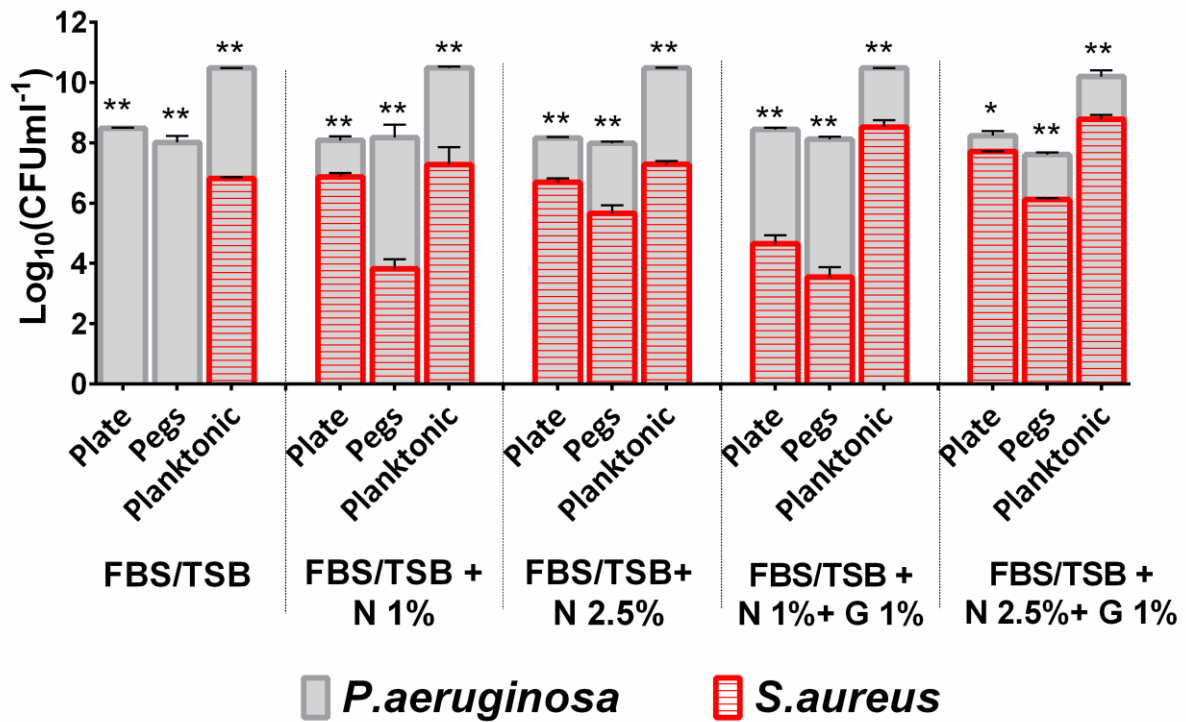
### 242 3.2 Media formulation for co-growth of *P. aeruginosa* and *S. aureus*

243 We finally chose TSB, as it is supporting growing media for *S. aureus*, and mixed it with FBS  
 244 (1:1)(Laura M Filkins et al., 2015), as we assumed that having some component from wound  
 245 area may support growth of dual species biofilms (Sun *et al*, 2008). We also enriched TSB with  
 246 NaCl and glucose to increase the chance of *S. aureus* to survive in the presence of *P. aeruginosa*  
 247 (Møretro et al., 2003; Waldrop et al., 2014). Finally, A 1:1 mixture of FBS and TSB or TSB  
 248 supplemented with 1% glucose, 2.5% NaCl, 1% NaCl, 1% glucose + 1% NaCl, 1% glucose +  
 249 2.5% NaCl were examined as growing media for dual species biofilm. Since biofilm assays are  
 250 often carried out in microtiter plates, either on the surface of plate wells or using peg-lids; both  
 251 biofilms formed on peg-lids and in plate wells were taken for CFU enumeration.

252 *P. aeruginosa* and *S. aureus* were inoculated in a volume ratio of 10:1, which lead to an equal  
 253 or higher CFU of *S. aureus* than *P. aeruginosa* in inoculation. We inoculated growth media  
 254 with a 10-time higher volume of *S. aureus* than *P. aeruginosa*, since CFU counting experiments  
 255 showed that *P. aeruginosa* grows about 1 log of CFU higher than *S. aureus* in both overnight

256 and 4 hours cultures. Co-culturing of two species in different enriched TSB indicated (Fig. 2)  
257 that *P. aeruginosa* forms biofilms in both plate wells and peg-lids in all five media  
258 formulations. In contrast, biofilm formation of *S. aureus* was not observed in TSB+FBS unless  
259 with addition of NaCl and glucose, which increased biofilm formation of *S. aureus* in both  
260 concentrations of 1% and 2.5%. TSB supplemented with 2.5% NaCl and glucose 1% mixed  
261 with FBS produced maximum biofilm growth of *S. aureus* (Fig. 2). The results are in agreement  
262 with previous studies, suggesting that the addition of NaCl and glucose to growth media  
263 promote biofilm formation by *S. aureus* (Waldrop *et al*, 2014; Lee *et al*, 2014). Glucose and  
264 NaCl increase biofilm formation of *S. aureus* by inducing expression levels of *icaA* gene (Lee  
265 *et al*, 2014; Møretrø *et al*, 2003; Rode *et al*, 2007). *IcaA* gene is strongly correlated to biofilm  
266 formation in staphylococcus species. *IcaA* encodes protein that cooperate in the synthesis of  
267 poly N-acetyl glucosamine, which mediates intercellular adhesion and accumulation of  
268 bacterial cells on the solid surfaces (Lin *et al.*, 2015). There are reports of the negative effect  
269 of NaCl on *P. aeruginosa* growth and biofilm formation (Michon *et al.*, 2014); however, we  
270 did not observe significant reduction of biofilm formation by *P. aeruginosa* in different media  
271 containing 0 to 2.5% NaCl. We also considered planktonic growth profile of each bacteria to  
272 have a full view of what takes place in each well. Planktonic growth of both species occurred  
273 in all tested media including simple TSB + FBS. Previous studies demonstrated that *P.*  
274 *aeruginosa* PAO1 can inhibit and disperse *S. aureus* biofilm through protease activity, while it  
275 has no bactericidal effect on its planktonic cell growth (Park *et al.*, 2012). The reason why *S.*  
276 *aureus* survive as planktonic in TSB+FBS and not in biofilm could also be explained by the  
277 fact that biofilm-resident cells have limited access to nutrition and/or oxygen, and thereby grow  
278 more slowly than planktonic cells (Donlan, 2001). It might make *S. aureus* biofilm cells more  
279 susceptible to *P. aeruginosa*. The higher inoculation volume of *S. aureus* than *P. aeruginosa*  
280 seemed to be necessary for *S. aureus* to survive in dual-species biofilm, which indicate that the

281 CFU number of *S. aureus* must be equal or more than *P. aeruginosa* for growing a dual species  
 282 biofilm. *S. aureus* killing by *P. aeruginosa* is a multifactorial phenomenon including  
 283 nutritional, genetic and environmental parameters, (Laura M. Filkins et al., 2015; Orazi and  
 284 O’Toole, 2017), thereby comprehensive studies are needed to elucidate interaction of these two  
 285 important species.



286

287 Figure 2: CFU counts of *P. aeruginosa* and *S. aureus*, co-cultured in FBS/TSB and FBS and  
 288 TSB supplemented with NaCl and glucose in different concentration after incubation for 24 h  
 289 at 37 °C. The concentration ratio of TSB/FBS for all growth media formulations was 50: 50.  
 290 Error bars indicate standard deviation (SD) from the mean of the 4 replicates. Two-way  
 291 ANOVA and Tukey’s multiple comparison tests were applied to analyze significance levels,

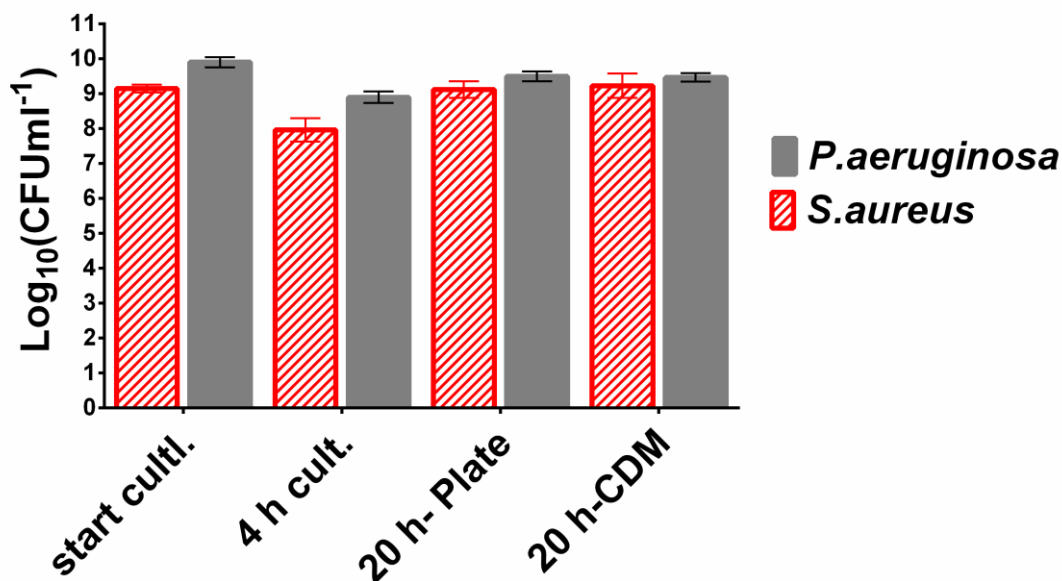
292 \* (P<0.01) and \*\* (P<0.001) indicate significant difference between *P. aeruginosa* and *S.*  
293 *aureus* CFU numbers.

### 294 **3.3 Dual-species biofilm on CDM**

295 Cell source is one of the main determinants of the composition of CDMs (Fitzpatrick and  
296 McDevitt, 2015). Different cell lines have been used to produce CDMs including fibroblasts,  
297 chondrocytes and mesenchymal stem cells (Lu et al., 2011). Fibroblast cells are major cell  
298 types involved in deposition of ECM and have a crucial role in the wound healing process  
299 (Tracy et al., 2016). Therefore, we used human dermal fibroblasts (HDF) cells as source cell  
300 to obtain a more relevant wound bed.

301 Dual-species biofilm was generated on CDMs in 24 well plates using FBS + TSB supplemented  
302 with 2.5%NaCl and 1% glucose (Fig. 3). Dual-species biofilm grown in wells without CDMs  
303 was used as control. Results did not reveal significant difference between growth rate of two  
304 bacterial species on surface of both CDMs and plates well (Fig. 3). The quantity of bacterial  
305 species co-cultured on CDMs after 24 hours was  $1.6 \times 10^9$  and  $2.9 \times 10^9$  CFU/ml for *P.*  
306 *aeruginosa* and *S. aureus*, respectively (Fig. 3).

307



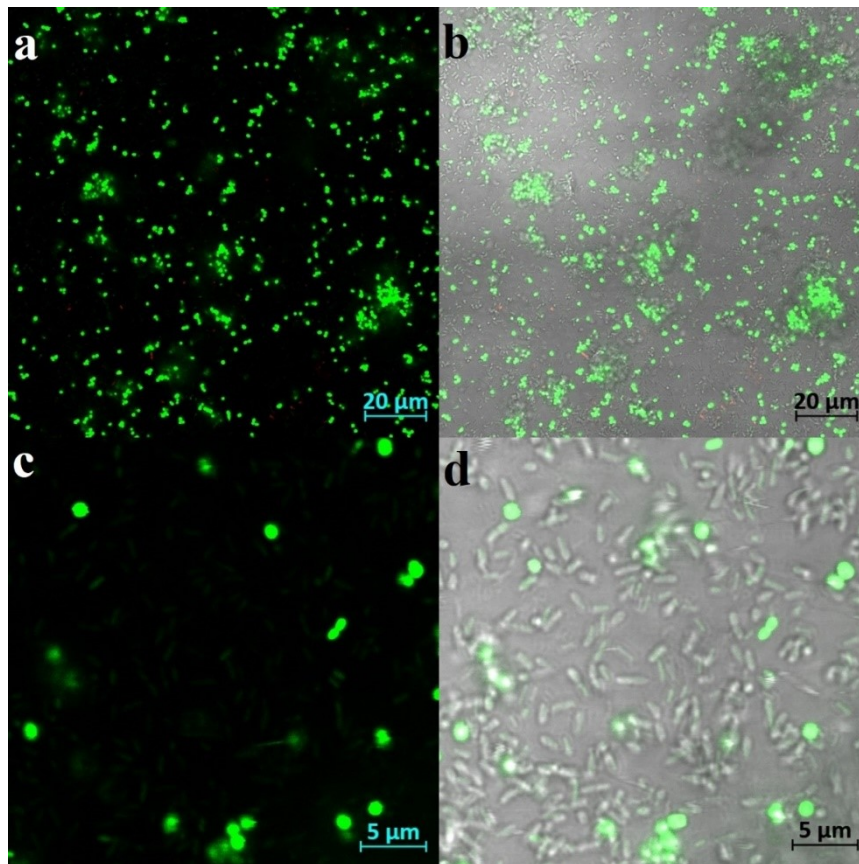
308

309 Figure 3. *P. aeruginosa* and *S. aureus* biofilm and planktonic populations. Start culture and 4  
 310 hours culture of both species was done in TSB media at 37°C and 180 rpm. Dual species  
 311 biofilms were grown in TSB enriched mixed with FBS (50:50) at 37°C. No significant  
 312 difference between *P. aeruginosa* and *S. aureus* CFU counts was observed. No significant  
 313 different of biofilm formation on CDM in compare to plate surface was obtained. Error bars  
 314 indicate standard deviation (SD) from the mean of the 4 replicates. Two-way ANOVA and  
 315 Tukey's multiple comparison tests were applied to analyze significance levels.

### 316 3.3 Characterization of the biofilm model

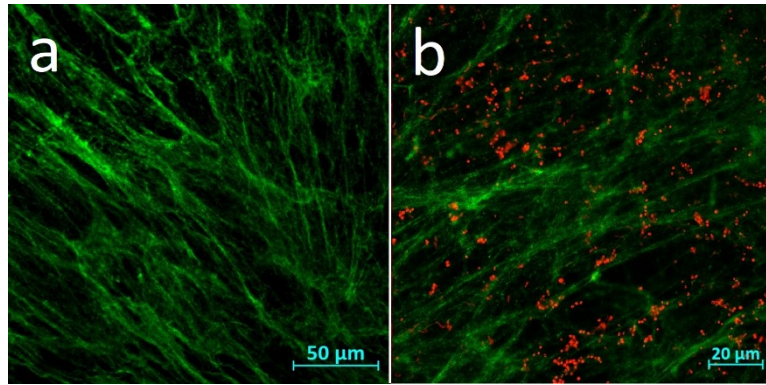
317 To visualize growth of bacterial species on the surface of CDMs, we examined biofilm with  
 318 live/dead assay (Fig. 4). The images showed both rod-shape *P. aeruginosa* and spherical-shape  
 319 *S. aureus* in the biofilm. The green fluorescence color, (indicating alive cells) was more  
 320 frequently observed for both species' cells than red fluorescence (indicating dead cells). As  
 321 presented in Fig. 5, CDMs organization and morphology was analyzed by immunofluorescence  
 322 staining. The fibrillary morphology of collagen type I and fibronectin can be seen in both  
 323 images of CDMs without and with biofilm. The thickness of the dual-species biofilm, formed  
 324 on CDMs, was about 6 μm, measured by Z-stack (Fig 6). The Z-stack planes revealed that *P.*

325 *aeruginosa* were more abundant in deeper layers of the biofilm and they could be seen inside  
326 the CDMs texture, while *S. aureus* cells were found more in the surface layers of the biofilm.  
327 This is in agreement with what have been described for wound samples from patients with non-  
328 healing diabetic ulcers in previous studies (Fazli *et al*, 2009; Peters *et al*, 2012). Although *P.*  
329 *aeruginosa* and *S. aureus* are two of the most frequent inhabitants of chronic wound biofilms,  
330 *P. aeruginosa* cells mostly distribute inside the wound bed while *S. aureus* cells are more  
331 located within the wound surface (Kirketerp-Møller *et al.*, 2008; Mulcahy *et al.*, 2015). This  
332 specific pattern of distribution could be attributed to several parameters. *P. aeruginosa* produce  
333 virulence factors which could disable activity of polymorphonuclear neutrophils, thereby  
334 helping *P. aeruginosa* to escape from killing by the immune system and penetrate into deeper  
335 layers of the wound bed (Kirketerp-Møller *et al.*, 2008). On the other hand, *P. aeruginosa* has  
336 polar type IV pili which make it able to migrate to deeper layers of the wound, where access to  
337 nutrition and space might be less competitive (Fazli *et al.*, 2009).



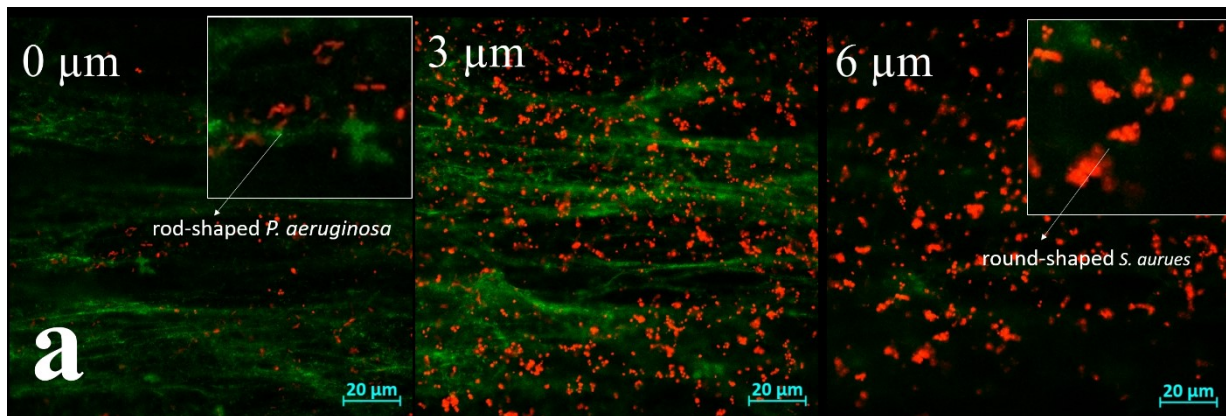
338

339 Figure 4: Fluorescence (a) and merged bright field (b) images of dual-species biofilm.  
340 Spherical *S. aureus* and rod-shaped *P. aeruginosa* of the surface of CDMs. Samples were  
341 stained with syto 9 as a membrane-permeant DNA-binding stain which indicate live cells as  
342 green and Propidium iodide as a red-fluorescent and nucleic acid-binding stain which penetrate  
343 damaged membrane and indicate dead cells. Images c and d show higher magnifications of a  
344 and b, respectively.



345

346 Figure 5: CDMs visualized by immunostaining of collagen I and fibronectins labeled in green  
 347 by Alexa Fluor 488 (a). Covered CDMs by dual-species biofilm (b), CDMs is visualized by  
 348 immunostaining of both collagen I and fibronectins labeled in green by Alexa Fluor 488 and  
 349 biofilm residents were visualized by propidium iodide (red dots).



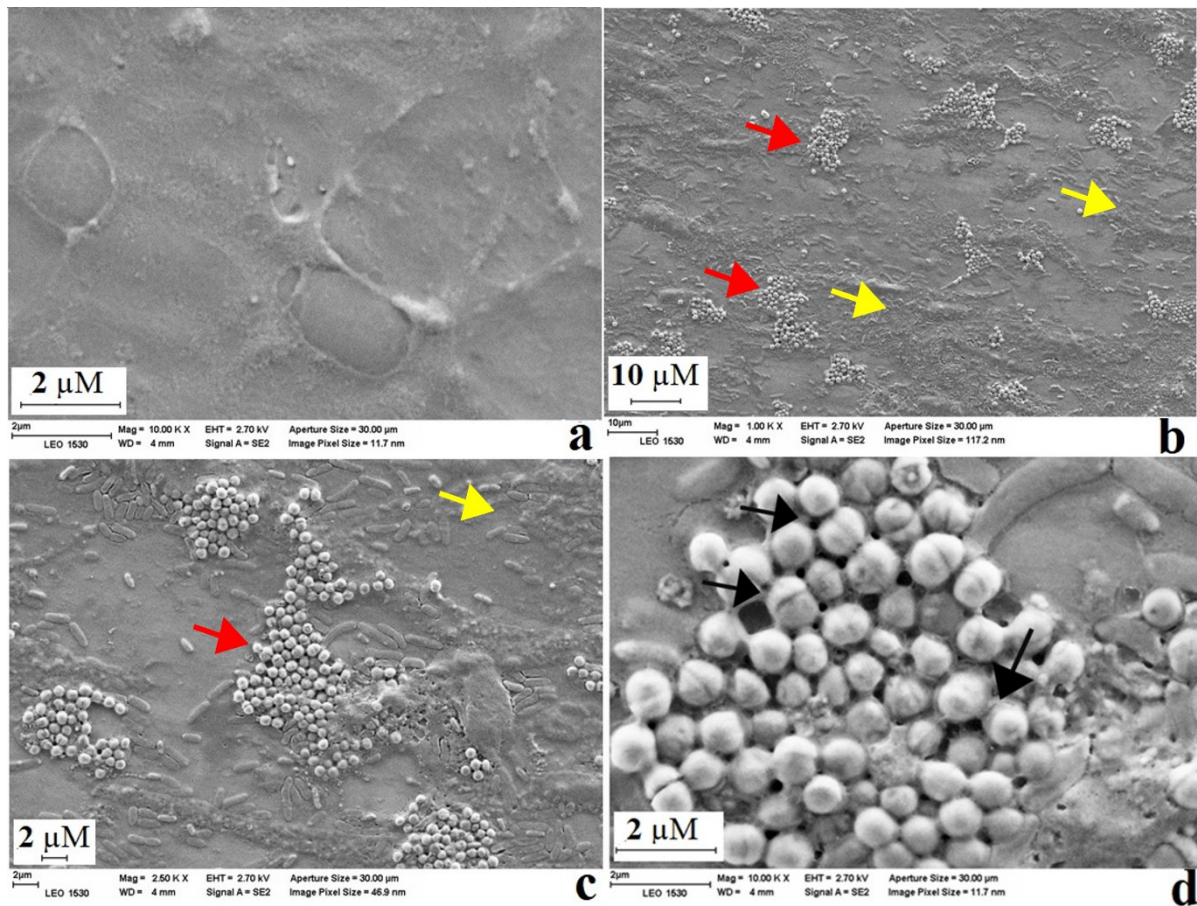
350

351 Figure 6: Selected pictures of z-stack planes of dual species biofilm on surface of CDMs. *P.*  
 352 *aeruginosa* cells are more frequent in the bottom layer of biofilms, while *S. aureus* cells were  
 353 seen more in surface layer of biofilm.

354 SEM images indicate a rough and fibrillary morphology for the surface of CDMs, in agreement  
 355 with previous studies (Kaukonen *et al*, 2017) (Fig. 7 a). Rod-shaped *P. aeruginosa* with a  
 356 length of 1-5 μm and width of 0.5-1 μm (Paterson and Kim, 2009) and spherical *S. aureus* with  
 357 a diameter of 0.5-1 μm (Harris *et al.*, 2002) were distinguishable in the SEM images (Fig. 7 b  
 358 and c).

359 *S. aureus* formed discrete compact colonies with 5-15  $\mu\text{m}$  diameter (analyzed using ImageJ  
360 image processing program, 1.47 v, National institutes of Health), while *P. aeruginosa* colonies  
361 were more spread over the biofilm (Figure 7 b and C). The inter-species interactions in the  
362 biofilm does not limit to inhibition or killing effects, but it also includes the impact on  
363 distribution pattern of bacterial species. *P. aeruginosa* induce *S. aureus* biofilm dispersal to  
364 compact colonies by making the environment less favorable for *S. aureus*. In the presented  
365 dual-species biofilm, *S. aureus* colonies also showed some of the properties of small colony  
366 variants (SCVs), including small and smooth colonies on mannitol salt agars and slow growing  
367 (data are not shown) (Hotterbeekx *et al*, 2017). Heterogeneous size of colonies and branched  
368 and multiple cross walls for *S. aureus* cells were observed in SEM images (Kah *et al.*, 2003;  
369 Lin *et al.*, 2016). One possible explanation for appearance of SCVs, may be due to anti-  
370 staphylococcal exoproduct of *P. aeruginosa*, HQNO and pyocyanin, which reduce growth of  
371 *S. aureus* by inhibition of oxidative respiration of bacteria (Hoffman *et al.*, 2006; Hotterbeekx  
372 *et al.*, 2017). SCVs are a survival mechanism of *S. aureus* that help it to escape from being  
373 killed by *P. aeruginosa*. SCVs are recovered from chronic infection of soft tissues like skin,  
374 bronchitis and mostly form cystic fibrosis (CF) chronic infection (Kriegeskorte *et al.*, 2015).  
375 SCVs are very challenging for treatment, since they are very difficult to be detected by routine  
376 microbiological methods, poorly sensitive to specific antibiotics and capable to acquire  
377 classical mechanisms of resistance to antibiotics, as normal *S.aureus* cells (Garcia *et al.*, 2013).  
378 Therefore, a reproducible biofilm model representing these abnormal phenotypes will be a  
379 useful tool to study their properties and their treatments.

380



381

382 Figure 7: Scanning electron images of surface of CDMs (a) and the biomimetic dual species

383 biofilm model (b and c). Red arrows show *S. aureus* and yellow arrows shows *P. aeruginosa*.

384 The images show the rough surface of CDMs and complex structure of dual-species biofilm

385 including SCV colonies. Arrows in image d indicate intercellular sticky substance among cells

386 and irregular cross cell walls present in SCVs as it was described by Lin et al. (Lin et al., 2016).

#### 387 4. Conclusion

388 In summary, we successfully established a dual-species biofilm on CDMs as an *in vitro* model

389 of wound infections. Using CDMs as a substrate for growing a dual species biofilm, the model

390 showed similar distribution patterns of two species in a chronic wound biofilm. The complex

391 distribution pattern of *P. aeruginosa* and *S. aureus* could compromise successful treatment of

392 biofilms existing in wounds, cystic fibrosis, as well as dental and surgical implant infections.

393 In these cases, high-throughput *in vitro* models could be practical alternatives to study the

394 interaction of biofilm residents. The obtained three-dimensional model has the potential to be  
395 employed for high-throughput screening of new antibacterial compounds and wound dressings.  
396 The model could further be useful in understanding the dynamic interaction of bacterial cells  
397 and biofilms with ECM components, which can provide valuable contribution to wound  
398 healing studies.

### 399 **Acknowledgements**

400 The authors acknowledge the Academy of Finland (grant no. 309374), Finnish National  
401 Agency for Education (EDUFI), Magnus Ehrnrooth and Sigrid Jusélius Foundations for  
402 financial support. Fang Cheng would further like to thank the National Natural Science  
403 Foundation of China (Grant no. 81702750) and the Basic Research Project of Shenzhen (Grant  
404 no. JCY20170818164756460) for funding cell tests. We also would like to thank Markku Saari  
405 and Jouko Sandholm of the Cell Imaging Core (CIC) at Turku, supported by Biocenter Finland,  
406 for technical support and advice.

### 407 **Conflicts of interest**

408 The authors declare no competing financial interest.

### 409 **References**

- 410 DeLeon, S., Clinton, A., Fowler, H., Everett, J., Horswill, A.R., Rumbaugh, K.P., 2014.  
411 Synergistic interactions of *Pseudomonas aeruginosa* and *Staphylococcus aureus* in an In  
412 vitro wound model. *Infect. Immun.* 82, 4718–4728. [https://doi.org/10.1128/IAI.02198-](https://doi.org/10.1128/IAI.02198-14)  
413 14
- 414 Donlan, R.M., 2001. Biofilm Formation: A Clinically Relevant Microbiological Process. *Clin.*  
415 *Infect. Dis.* 33, 1387–1392. <https://doi.org/10.1086/322972>
- 416 Fazli, M., Bjarnsholt, T., Kirketerp-Møller, K., Jørgensen, B., Andersen, A.S., Krogfelt, K.A.,

417 Givskov, M., Tolker-Nielsen, T., 2009. Nonrandom distribution of *Pseudomonas*  
418 *aeruginosa* and *Staphylococcus aureus* in chronic wounds. *J. Clin. Microbiol.* 47, 4084–  
419 4089. <https://doi.org/10.1128/JCM.01395-09>

420 Filkins, Laura M., Graber, J.A., Olson, D.G., Dolben, E.L., Lynd, L.R., Bhujju, S., O’Toole, G.A.,  
421 2015. Coculture of *Staphylococcus aureus* with *Pseudomonas aeruginosa* drives *S.*  
422 *aureus* towards fermentative metabolism and reduced viability in a cystic fibrosis  
423 model. *J. Bacteriol.* 197, 2252–2264. <https://doi.org/10.1128/JB.00059-15>

424 Filkins, Laura M, Graber, J.A., Olson, D.G., Dolben, E.L., Lynd, L.R., Bhujju, S., Toole, A.O.,  
425 2015. Coculture of *Staphylococcus aureus* with *Pseudomonas aeruginosa* Drives *S.*  
426 *aureus* towards Fermentative Metabolism and Reduced Viability in a Cystic Fibrosis  
427 Model 197, 2252–2264. <https://doi.org/10.1128/JB.00059-15>

428 Fitzpatrick, L.E., McDevitt, T.C., 2015. Cell-derived matrices for tissue engineering and  
429 regenerative medicine applications. *Biomater. Sci.* 3, 12–24.  
430 <https://doi.org/10.1039/c4bm00246f>

431 Frykberg, R.G., Banks, J., 2015. Challenges in the Treatment of Chronic Wounds. *Adv. Wound*  
432 *Care* 4, 560–582. <https://doi.org/10.1089/wound.2015.0635>

433 Garcia, L.G., Lemaire, S., Kahl, B.C., Becker, K., Proctor, R.A., Denis, O., Tulkens, P.M., Van  
434 Bambeke, F., 2013. Antibiotic activity against small-colony variants of *staphylococcus*  
435 *aureus*: Review of in vitro, animal and clinical data. *J. Antimicrob. Chemother.* 68,  
436 1455–1464. <https://doi.org/10.1093/jac/dkt072>

437 Han, G., Ceilley, R., 2017. Chronic Wound Healing: A Review of Current Management and  
438 Treatments. *Adv. Ther.* 34, 599–610. <https://doi.org/10.1007/s12325-017-0478-y>

439 Harris, L.G., Foster, S.J., Richards, R.G., Lambert, P., Stickler, D., Eley, A., 2002. An  
440 introduction to *Staphylococcus aureus*, and techniques for identifying and quantifying *S.*  
441 *aureus* adhesins in relation to adhesion to biomaterials: Review. *Eur. Cells Mater.* 4, 39–  
442 60. <https://doi.org/10.22203/eCM.v004a04>

443 Hoffman, L.R., Deziel, E., D'Argenio, D.A., Lepine, F., Emerson, J., McNamara, S., Gibson, R.L.,  
444 Ramsey, B.W., Miller, S.I., 2006. Selection for *Staphylococcus aureus* small-colony  
445 variants due to growth in the presence of *Pseudomonas aeruginosa*. *Proc. Natl. Acad.*  
446 *Sci.* 103, 19890–19895. <https://doi.org/10.1073/pnas.0606756104>

447 Hotterbeekx, A., Kumar-Singh, S., Goossens, H., Malhotra-Kumar, S., 2017. In vivo and In  
448 vitro Interactions between *Pseudomonas aeruginosa* and *Staphylococcus* spp. *Front.*  
449 *Cell. Infect. Microbiol.* 7, 1–13. <https://doi.org/10.3389/fcimb.2017.00106>

450 Kah, B.C., Belling, G., Reichelt, R., Herrmann, M., Proctor, R.A., Peters, G., 2003. Thymidine-  
451 Dependent Small-Colony Variants of *Staphylococcus aureus* Exhibit Gross  
452 Morphological and Ultrastructural Changes Consistent with Impaired Cell Separation. *J.*  
453 *Clin. Microbiol.* 41, 301–304. <https://doi.org/10.1128/JCM.41.1.410>

454 Kaukonen, R., Jacquemet, G., Hamidi, H., Ivaska, J., 2017. Cell-derived matrices for studying  
455 cell proliferation and directional migration in a complex 3D microenvironment. *Nat.*  
456 *Protoc.* 12, 2376–2390. <https://doi.org/10.1038/nprot.2017.107>

457 Kirketerp-Møller, K., Jensen, P., Fazli, M., Madsen, K.G., Pedersen, J., Moser, C., Tolker-  
458 Nielsen, T., Høiby, N., Givskov, M., Bjarnsholt, T., 2008. Distribution, organization, and  
459 ecology of bacteria in chronic wounds. *J. Clin. Microbiol.* 46, 2717–2722.  
460 <https://doi.org/10.1128/JCM.00501-08>

461 Kriegeskorte, A., Lorè, I., Bragonzi, A., Riva, C., Kelkenberg, M., Becker, K., Proctor, R.A.,  
462 Peters, G., Kahl, C., 2015. Are Induced by Trimethoprim-Sulfamethoxazole ( SXT ) and  
463 Have Increased Fitness during SXT Challenge 59, 7265–7272.  
464 <https://doi.org/10.1128/AAC.00742-15>.Address

465 Kucera, J., Sojka, M., Pavlik, V., Szuszkiewicz, K., Velebny, V., Klein, P., 2014. Multispecies bio  
466 film in an artificial wound bed — A novel model for in vitro assessment of solid  
467 antimicrobial dressings. J. Microbiol. Methods 103, 18–24.  
468 <https://doi.org/10.1016/j.mimet.2014.05.008>

469 Lee, S., Choi, K., Yoon, Y., 2014. Effect of NaCl on Biofilm Formation of the Isolate from  
470 Staphylococcus aureus Outbreak Linked to Ham. Korean J. Food Sci. Anim. Resour. 34,  
471 257–261. <https://doi.org/10.5851/kosfa.2014.34.2.257>

472 Lin, M.H., Shu, J.C., Lin, L.P., Chong, K. yu, Cheng, Y.W., Du, J.F., Liu, S.-T., 2015. Elucidating  
473 the Crucial Role of Poly N-Acetylglucosamine from Staphylococcus aureus in Cellular  
474 Adhesion and Pathogenesis. PLoS One 10, e0124216.  
475 <https://doi.org/10.1371/journal.pone.0124216>

476 Lin, Y.-T., Tsai, J.-C., Yamamoto, T., Chen, H.-J., Hung, W.-C., Hsueh, P.-R., Teng, L.-J., 2016.  
477 Emergence of a small colony variant of vancomycin-intermediate *Staphylococcus*  
478 *aureus* in a patient with septic arthritis during long-term treatment with daptomycin. J.  
479 Antimicrob. Chemother. 71, 1807–1814. <https://doi.org/10.1093/jac/dkw060>

480 Lipsky, B.A., Hoey, C., 2009. Topical Antimicrobial Therapy for Treating Chronic Wounds.  
481 Clin. Infect. Dis. 49, 1541–1549. <https://doi.org/10.1086/644732>

482 Lu, H., Hoshiba, T., Kawazoe, N., Chen, G., 2011. Autologous extracellular matrix scaffolds

483 for tissue engineering. *Biomaterials* 32, 2489–2499.  
484 <https://doi.org/10.1016/j.biomaterials.2010.12.016>

485 Magana, M., Sereti, C., Ioannidis, A., Mitchell, C.A., Ball, A.R., Magiorkinis, E.,  
486 Chatzipanagiotou, S., Hamblin, M.R., Hadjifrangiskou, M., Tegos, G.P., 2018. Options  
487 and Limitations in Clinical Investigation of Bacterial Biofilms. *Clin. Microbiol. Rev.* 31,  
488 e00084-16. <https://doi.org/10.1128/CMR.00084-16>

489 Mathes, S.H., Ruffner, H., Graf-Hausner, U., 2014. The use of skin models in drug  
490 development. *Adv. Drug Deliv. Rev.* 69–70, 81–102.  
491 <https://doi.org/10.1016/j.addr.2013.12.006>

492 McCarty, S.M., Percival, S.L., 2013. Proteases and Delayed Wound Healing. *Adv. WOUND*  
493 *CARE* 2, 438–447. <https://doi.org/10.1089/wound.2012.0370>

494 Michon, A.L., Jumas-Bilak, E., Chiron, R., Lamy, B., Marchandin, H., 2014. Advances toward  
495 the elucidation of hypertonic saline effects on *Pseudomonas aeruginosa* from cystic  
496 fibrosis patients. *PLoS One* 9, 1–8. <https://doi.org/10.1371/journal.pone.0090164>

497 Mørretrø, T., Hermansen, L., Holck, A.L., Sidhu, M.S., Rudi, K., Langsrud, S., 2003. Biofilm  
498 formation and the presence of the intercellular adhesion locus *ica* among staphylococci  
499 from food and food processing environments. *Appl. Environ. Microbiol.* 69, 5648–5655.  
500 <https://doi.org/10.1128/AEM.69.9.5648-5655.2003>

501 Mulcahy, L.R., Isabella, V.M., Lewis, K., 2015. *Pseudomonas aeruginosa* biofilms in disease.  
502 *Microb. Ecol.* 68, 1–12. <https://doi.org/10.1007/s00248-013-0297-x>. *Pseudomonas*

503 Orazi, G., O’Toole, G.A., 2017. *Pseudomonas aeruginosa* alters *Staphylococcus aureus*  
504 sensitivity to vancomycin in a biofilm model of cystic fibrosis infection. *MBio* 8, 1–17.

505 <https://doi.org/10.1128/mBio.00873-17>

506 Park, J.H., Lee, J.H., Cho, M.H., Herzberg, M., Lee, J., 2012. Acceleration of protease effect on  
507 *Staphylococcus aureus* biofilm dispersal. *FEMS Microbiol. Lett.* 335, 31–38.  
508 <https://doi.org/10.1111/j.1574-6968.2012.02635.x>

509 Paterson, D.L., Kim, B.-N., 2009. *Pseudomonas aeruginosa*, in: *Antimicrobial Drug*  
510 *Resistance*. Humana Press, Totowa, NJ, pp. 811–817. [https://doi.org/10.1007/978-1-](https://doi.org/10.1007/978-1-60327-595-8_9)  
511 [60327-595-8\\_9](https://doi.org/10.1007/978-1-60327-595-8_9)

512 Peters, B.M., Jabra-Rizk, M.A., O'May, G.A., William Costerton, J., Shirtliff, M.E., 2012.  
513 *Polymicrobial interactions: Impact on pathogenesis and human disease*. *Clin. Microbiol.*  
514 *Rev.* 25, 193–213. <https://doi.org/10.1128/CMR.00013-11>

515 Rode, T.M., Langsrud, S., Holck, A., Møretrø, T., 2007. Different patterns of biofilm  
516 formation in *Staphylococcus aureus* under food-related stress conditions. *Int. J. Food*  
517 *Microbiol.* 116, 372–383. <https://doi.org/10.1016/j.ijfoodmicro.2007.02.017>

518 Sahlgren, C., Meinander, A., Zhang, H., Cheng, F., Preis, M., Xu, C., Salminen, T.A., Toivola,  
519 D., Abankwa, D., Rosling, A., Karaman, D.Ş., Salo-Ahen, O.M.H., Österbacka, R.,  
520 Eriksson, J.E., Willför, S., Petre, I., Peltonen, J., Leino, R., Johnson, M., Rosenholm, J.,  
521 Sandler, N., 2017. Tailored Approaches in Drug Development and Diagnostics: From  
522 Molecular Design to Biological Model Systems. *Adv. Healthc. Mater.* 6, 1700258.  
523 <https://doi.org/10.1002/adhm.201700258>

524 Sun, Y., Dowd, S.E., Smith, E., Rhoads, D.D., Wolcott, R.D., 2008. In vitro multispecies  
525 Lubbock chronic wound biofilm model. *Wound Repair Regen.* 16, 805–813.  
526 <https://doi.org/10.1111/j.1524-475X.2008.00434.x>

527 Tracy, L.E., Minasian, R.A., Caterson, E.J., 2016. Extracellular Matrix and Dermal Fibroblast  
528 Function in the Healing Wound. *Adv. Wound Care* 5, 119–136.  
529 <https://doi.org/10.1089/wound.2014.0561>

530 Waldrop, R., McLaren, A., Calara, F., McLemore, R., 2014. Biofilm Growth Has a Threshold  
531 Response to Glucose in Vitro. *Clin. Orthop. Relat. Res.* 472, 3305–3310.  
532 <https://doi.org/10.1007/s11999-014-3538-5>

533 Werthe, M., Henriksson, L., Jensen, P.Ø., Sternberg, C., Givskov, M., Bjarnsholt, T., 2010. An  
534 in vitro model of bacterial infections in wounds and other soft tissues. *APMIS* 156–164.  
535 <https://doi.org/10.1111/j.1600-0463.2009.02580.x>

536 Zeng, G., Vad, B.S., Dueholm, M.S., Christiansen, G., Nilsson, M., Tolker-Nielsen, T., Nielsen,  
537 P.H., Meyer, R.L., Otzen, D.E., 2015. Functional bacterial amyloid increases  
538 *Pseudomonas* biofilm hydrophobicity and stiffness. *Front. Microbiol.* 6, 1–14.  
539 <https://doi.org/10.3389/fmicb.2015.01099>

540

541